Prepared for submission to XXX

# Linear Resistivity from Spatially Random Interactions and the Uniqueness of Yukawa Coupling

**Sang-Jin Sin,** [a] **Yi-Li Wang**[a,b]

[a] *Department of Physics, Hanyang University, 222 Wangsimni-ro, Seoul, 04763, Korea*
[b] *Asia Pacific Center for Theoretical Physics, 77 Cheongam-ro, Pohang, 37673, Korea*

*E-mail:* sjsin@hanyang.ac.kr, yili.wang@apctp.org

Abstract: Recent studies have shown that a spatially random Yukawa-type interaction between a Fermi surface and critical bosons can produce linear-in-temperature resistivity, the defining signature of strange metals. In this article, we systematically classify all scalar couplings of the form $(\psi^\dagger\psi)^n\phi^m$ in arbitrary dimensions to identify possible candidates for strange-metal behaviour within this disordered framework. We find that only spatially random Yukawa-type interaction in $(2+1)$ dimensions can yield linear resistivity.

## Contents



## 1 Introduction

Strange metals have been recognized as one of the central topics in modern physics [1–7]. As the normal phase of superconductors, strange metals exhibit striking deviations from the Landau Fermi liquid theory. A defining feature of strange metals is linear-$T$ resistivity, $\rho \sim \rho_0 + AT$, where $\rho_0$ is the residual resistivity and $A$ is a material-dependent coefficient. Despite extensive efforts over the past several decades, a systematic understanding of strange remains absent. A major obstacle is the lack of a theoretical framework accounting for the anomalous transport properties of strange metals, particularly the origin of linear resistivity.

Recently, Patel *et al.* [8] introduced a spatially random coupling between a Fermi surface and a critical scalar boson, described by the interaction

$$S_{\text{int}} = \int d\tau d^2\boldsymbol{r} \sum_{i,j,l=1}^{N} \frac{g_{ijl}(\boldsymbol{r})}{N} \psi_i^\dagger(\tau,\boldsymbol{r})\psi_j(\tau,\boldsymbol{r})\phi_l(\tau,\boldsymbol{r}). \tag{1.1}$$

The coupling constant $g_{ijl}(\boldsymbol{r})$ follows a Gaußian distribution with zero mean and variance $\langle g^*_{ijl}(\boldsymbol{r})g_{i'j'l'}(\boldsymbol{r}')\rangle = g^2\delta(\boldsymbol{r}-\boldsymbol{r}')\delta_{ii',jj',ll'}$. It was pointed out in ref.[9] that in this space dependent random coupling's variance condition provides a wormhole picture in the field theory, which make it possible for far separated point to interact without distance dependent suppression. At large-$N$ limit, this quenched disorder leads to linear resistivity at low temperatures. Subsequently, it was shown that the same strange metal transport property arises under an annealed average [9], and that the equivalence between quenched and annealed averages can be viewed as a concrete realisation of the $ER = EPR$ conjecture [10]. This is different from the case where spatially homogeneous case which does not admit wormhole picture nor the strange metalicity. Furthermore, while the wormhole picture in the original SYK model is in the holographic spacetime and half circumstantial, our field theory wormhole is directly that of the original spacetime and it does not need any higher dimensional structure, because it is a direct consequence of the Gaussian average of the spatial random coupling.

A similar fully randomised QED-like coupling between the critical Fermi surface and a vector boson can also reproduce such a linearity [11], even in the presence of a magnetic field [12]. These all-to-all spatially random interactions, inspired by the Sachdev-Ye-Kitaev (SYK) model [13–15], are referred to as 'SYK-rised' models in this article. Although such couplings cannot capture other anomalies of strange metals, such as Hall angles [12], they currently offer the only known mechanism that produces linear resistivity in a controlled, analytically tractable setting.

SYK-rised models offer a promising route to understanding the nature of strange metals. This raises a natural question: *what is most general types of random interactions between the FS and the critical boson also give rise to linear resistivity?* In addition to higher-rank tensor couplings, one may consider interactions involving multiple fields. Since the theory use the critical fluctuations, we will investigate the SYK-rised interaction of the type $(\psi^\dagger\psi)^n\phi^m$ which does not generate mass scale, and investigate the possibility that leads to linear-in-temperature resistivity across various spacetime dimensions. We find that the original Yukawa-type couplings are the only class that produces linear-$T$ resistivity.

This article is organised as follows. Section 2 develops a large-$N$ critical theory of spatial random couplings involving arbitrary numbers of fermions and bosons. The corresponding conductivity is calculated in section 3. Concluding remarks are given in Section 5.

## 2 Generalised Spatially Random Coupling

### 2.1 $G-\Sigma$ formalism

We begin by reviewing the model introduced in ref.[8], which provides the first theoretical realisation of linear-in-temperature resistivity. The fermionic field $\psi_i$ and scalar field $\phi_i$

are described by standard kinetic terms,

$$S_0 = \int d\tau \sum_{\boldsymbol{k}} \sum_{i=1}^{N} \psi^\dagger_{i\boldsymbol{k}}(\tau) \left[\partial_\tau + \varepsilon(\boldsymbol{k}) - \mu\right] \psi_{i\boldsymbol{k}}(\tau) + \int d\tau d^2\boldsymbol{r} \psi^\dagger_i(\tau,\boldsymbol{r}) v_{ij}(\boldsymbol{r}) \psi_j(\tau,\boldsymbol{r})$$
$$+\frac{1}{2}\int d\tau \sum_{\boldsymbol{q}} \sum_{i=1}^{N} \phi_{i\boldsymbol{q}}(\tau) \left[-\partial_\tau^2 + \boldsymbol{q}^2 + m_b^2\right] \phi_{i,-\boldsymbol{q}}(\tau), \tag{2.1}$$

where $i = 1, ..., N$ denotes the flavour index. The potential disorder $v_{ij}$ is introduced with Gaußian statistics,

$$\langle v_{ij}(\boldsymbol{r})\rangle = 0\,, \quad \langle v^*_{ij}(\boldsymbol{r}) v_{lm}(\boldsymbol{r}')\rangle = v^2\,\delta(\boldsymbol{r}-\boldsymbol{r}')\delta_{il}\delta_{jm}. \tag{2.2}$$

The key ingredient is a quenched disorder interaction between electrons and bosons,

$$S_{\text{int}} = \int d\tau d^2\boldsymbol{r} \sum_{i,j,l=1}^{N} \frac{g_{ijl}(\boldsymbol{r})}{N} \psi^\dagger_i(\boldsymbol{r}) \psi_j(\boldsymbol{r}) \phi_l(\boldsymbol{r},\tau), \tag{2.3}$$

with the coupling constants satisfying

$$\langle g_{jil}(\boldsymbol{r})\rangle = 0, \quad \langle g^*_{ijl}(\boldsymbol{r}) g_{i'j'l'}(\boldsymbol{r}')\rangle = g^2 \delta_{ii'jj'll'}\delta(\boldsymbol{r}-\boldsymbol{r}'). \tag{2.4}$$

We refer to the interaction (2.4) as an 'SYK-rised' Yukawa coupling, as it describes a spatially random all-to-all interaction analogous to the SYK model. It has been shown that in the large-$N$ limit, this interaction yields linear resistivity at low temperatures. Moreover, such SYK-rised mechanism remains effective when extended to vector bosons [11]. It is our interest to figure out whether this is the *unique* scalar coupling that leads to linear resistivity, and whether such behaviour persists in higher-dimensional systems.

A generalisation of interaction (2.4) is to increase the number of fields. Specifically, we consider an interaction fo the form

$$S_g = \frac{g_{\{i\}\{j\}\{l\}}(\boldsymbol{r})}{N^{(2n+m-1)/2}} \int d\tau d^d r \sum_{\{i\},\{j\},\{l\}} \psi^\dagger_{i_1,\boldsymbol{k}}(\boldsymbol{r},\tau)...\psi^\dagger_{i_n,\boldsymbol{k}}(\boldsymbol{r},\tau)$$
$$\times\, \psi_{j_1,\boldsymbol{k}+\boldsymbol{q}}(\boldsymbol{r},\tau)...\psi_{j_n,\boldsymbol{k}+\boldsymbol{q}}(\boldsymbol{r},\tau)\phi_{l_1,\boldsymbol{q}}(\boldsymbol{r},\tau)...\phi_{l_m,\boldsymbol{q}}(\boldsymbol{r},\tau), \tag{2.5}$$

with $d \geq 2$. The vertex involves $2n$ fermionic fields and $m$ bosonic fields, whilst the coupling constant $g_{\{i\}\{j\}\{l\}} \equiv g_{i_1...i_n j 1...j_n l_1...l_m}$ obeys Gaußian distribution,

$$\langle g_{\{i\}\{j\}\{l\}}(\boldsymbol{r})\rangle = 0, \tag{2.6}$$
$$\langle g_{\{i\}\{j\}\{l\}}(\boldsymbol{r}) g^*_{\{i'\}\{j'\}\{l'\}}(\boldsymbol{r}')\rangle = g^2\delta(\boldsymbol{r}-\boldsymbol{r}')\delta_{\{i\}\{i'\},\{j\}\{j'\},\{l\}\{l'\}}, \tag{2.7}$$

with multi-index delta functions defined by

$$\delta_{\{i\}\{i'\}} \equiv \delta_{i_1 i'_1}\delta_{i_2 i'_2}...\delta_{i_n i'_n}. \tag{2.8}$$

Instead of working in $(2+1)$ dimensions, we consider general $(d+1)$D systems to find the effect of dimensionality.

We now derive the $G-\Sigma$ action of theory (2.5). We define bilocal variables

$$G(x_1,x_2) \equiv -\frac{1}{N}\sum_{i=1}^{N}\psi_i(x_1)\psi_i^\dagger(x_2), \tag{2.9}$$

$$D(x_1,x_2) \equiv \frac{1}{N}\sum_{i=1}^{N}\phi_i(x_1)\phi_i(x_2), \tag{2.10}$$

and impose them via Lagrange multipliers. This gives rise to the term

$$\begin{aligned} S_L = &-N\int d\tau d\tau' \sum_k \Sigma(\boldsymbol{k},\tau'-\tau)\left[G(\boldsymbol{k},\tau-\tau') + \frac{1}{N}\sum_{i=1}^{N}\psi_{i,\boldsymbol{k}}(\tau)\psi^\dagger_{i,\boldsymbol{k}}(\tau')\right] \\ &+\frac{N}{2}\int d\tau d\tau' \sum_q \Pi(\boldsymbol{q},\tau'-\tau)\left[D(\boldsymbol{q},\tau-\tau') - \frac{1}{N}\sum_{i=1}^{N}\phi_{i,\boldsymbol{q}}(\tau)\phi_{i,-\boldsymbol{q}}(\tau')\right]. \end{aligned} \tag{2.11}$$

Following the analysis in Ref.[16], we neglect the replica off-diagonal components of $G(x_1,x_2)$ and $D(x_1,x_2)$ in large $N$. As emphasised in ref.[16, 18], the universal properties of critical theories are expected to be insensitive to the microscopic details of the interaction. We therefore assume replica symmetry from the outset.

Then we perform the disorder average using the replica trick. The partition function is given by

$$\mathcal{Z} \equiv \int \mathcal{D}[\psi,\psi^\dagger]\mathcal{D}[\phi]e^{-S_0-S_g-S_{\rm L}}, \tag{2.12}$$

and the resulting Gaußian integrals can be evaluated as

$$\int \mathcal{D}[\psi,\psi^\dagger]e^{-\psi^\dagger\mathbf{A}\psi} = \det\mathbf{A}, \tag{2.13}$$

$$\int \mathcal{D}[\phi]e^{-\phi\mathbf{A}\phi/2} = \det\mathbf{A}^{-1/2}. \tag{2.14}$$

Applying these to the replicated action yields the effective action

$$\begin{aligned} \frac{S[G,\Sigma;D,\Pi]}{N} = &-\ln\det\left(\partial_\tau + \varepsilon(\boldsymbol{k})\delta(x-x') - \mu + \Sigma\right) \\ &+\frac{1}{2}\ln\det\left(\left(-\partial_\tau^2 + K\boldsymbol{q}^2 + m_b^2\right)\delta(x-x') - \Pi\right) \\ &-\mathrm{Tr}\left(\Sigma\cdot G\right) + \frac{1}{2}\mathrm{Tr}\left(\Pi\cdot D\right) + \frac{v^2}{2}\mathrm{Tr}\left((G\bar{\delta})\cdot G\right) \\ &+(-1)^{n^2+1}\frac{g^2}{2}\mathrm{Tr}\left((G^nD^m\bar{\delta})\cdot(G)^n\right), \end{aligned} \tag{2.15}$$

where $\bar{\delta}$ is a Dirac delta over space, $\delta(\boldsymbol{r}-\boldsymbol{r}')$, and the trace notation is defined by [19]

$$\mathrm{Tr}(f\cdot g) \equiv f^T g \equiv \int dx_1 dx_2 f(x_2,x_1)g(x_1,x_2)\,. \tag{2.16}$$

Assuming replica symmetry, we drop replica indices without loss of generality.

### 2.2 Large-$N$ Critical Theory

The large-$N$ limit is governed by the saddle point of the $G-\Sigma$ action (2.15). Varying the action yields

$$\begin{aligned} 0 &= \frac{\delta S}{N} \\ &= \mathrm{Tr}\left(\delta\Sigma\cdot(G_*[\Sigma]-G)+\delta G\cdot(\Sigma_*[G]-\Sigma)+\frac{1}{2}\delta\Pi\cdot(D-D_*[\Pi])+\frac{1}{2}\delta D\cdot(\Pi-\Pi_*[D])\right). \end{aligned} \tag{2.17}$$

Using the identity

$$\ln\det\mathbf{M}=\mathrm{Tr}\ln\mathbf{M},\qquad \delta\left[\ln\det\mathbf{M}\right]=\mathrm{Tr}\left[\mathbf{M}^{-1}\delta\mathbf{M}\right], \tag{2.18}$$

we obtain the saddle-point equations (Schwinger-Dyson equations),

$$G_*[\Sigma](x_1,x_2) = (-\partial_\tau-\varepsilon(\boldsymbol{k})+\mu-\Sigma)^{-1}(x_1,x_2), \tag{2.19}$$

$$\Sigma_*[G](x_1,x_2) = (-1)^{n^2+1}ng^2G^{2n-1}(x_1,x_2)D^m(x_1,x_2)\bar{\delta}+v^2G(x_1,x_2)\bar{\delta}, \tag{2.20}$$

$$D_*[\Pi](x_1,x_2) = (-\partial_\tau^2+K\boldsymbol{q}^2+m_b^2-\Pi)^{-1}(x_1,x_2), \tag{2.21}$$

$$\Pi_*[D](x_1,x_2) = mg^2G^{2n}(x_1,x_2)D^{m-1}(x_1,x_2)\bar{\delta}. \tag{2.22}$$

Setting $n=m=1$ recovers the saddle-point structure of the SYK-rised Yukawa model discussed in Refs.[8, 16, 20]. We adopt the conventional quadratic dispersion $\varepsilon(\boldsymbol{k})=\boldsymbol{k}^2/(2m)$, and fix units such that the boson velocity $\sqrt{K}=1$.

The next step is to solve these Schwinger-Dyson equations at $T=0$. To simplify the calculation, we define $\xi_{\boldsymbol{k}}\equiv\varepsilon(\boldsymbol{k})-\mu$. The contribution from potential disorder $v_{ij}(\boldsymbol{r})$ is

$$\begin{aligned} \Sigma_v(\Omega_m) &= v^2\int\frac{d^d\boldsymbol{k}}{(2\pi)^2}G(i\Omega_m,\boldsymbol{k}) \\ &= v^2\mathcal{N}\int d\xi_{\boldsymbol{k}}\frac{1}{i\Omega_m-\xi_{\boldsymbol{k}}-\Sigma(i\Omega_m,\boldsymbol{k})} \\ &= -i\frac{\Gamma}{2}\mathrm{sgn}(\Omega_m), \end{aligned} \tag{2.23}$$

where $\mathcal{N}$ is the fermion density of states *at the Fermi level* in $d$-space, and $\Gamma=2\pi v^2\mathcal{N}$ denotes the disorder scattering rate [21]. In the last step, we have used the fact that $\mathrm{sgn}(\omega_n)=-\mathrm{sgn}(\mathrm{Im}\{\Sigma(\mathrm{i}\omega_n)\})$.

We now assume that impurity scattering dominates over interactions, *i.e.* $|\Sigma_v|\gg|\Sigma_g|$, so that the electron propagator is well approximated by potential disorder alone. At low frequencies,

$$G(\mathrm{i}\omega,\boldsymbol{k})\simeq\frac{1}{\mathrm{isgn}(\omega)\Gamma/2-\boldsymbol{k}^2/(2m)+\mu}, \tag{2.24}$$

where the corrections from fermion-boson coupling are suppressed at leading order.


(a) Bosonic self-energy (b) Fermionic self-energy

**Figure 1**: Two self-energies, $\Pi$ and $\Sigma$, share the same structure.

At critical point, the boson mass satisfies $m_b^2 - \Pi(0,0) = 0$ [16]. The full bosonic propagator can be expressed as

$$D(\mathrm{i}\Omega_m, \boldsymbol{q}) = \frac{1}{\Omega_m^2 + \boldsymbol{q}^2 - (\Pi - \Pi(\Omega_m = 0))}. \tag{2.25}$$

It remains to evaluate $\Pi(\mathrm{i}\Omega) - \Pi(0,0)$, which encodes the leading dynamical correction to the critical bosonic propagator.

We now turn to the evaluation of the self-energies. The boson self-energy (2.22) is graphically represented by Fig.1a, where solid lines denote fermion propagators, wavy lines denote bosons, and dashed lines indicate disorder averaging. The fermionic self-energy (2.20) is illustrated in Fig.1b. Since bosonic self-energy and bosonic self-energy are structurally similar, we do not need to compute them separately. Instead, we can analyse both simultaneously by studying the frequency dependence of a generic diagram containing $\alpha$ fermion lines and $\beta$ boson lines. [1]

### 2.2.1 Scaling Behaviour from Dimensional Considerations

Before delving into the full calculation, we first provide a heuristic estimate of the self-energies using dimensional analysis.

The fermionic Green's function is approximately given by eqn.(2.24), but bosonic propagator remains undetermined. As a result, generic diagrams with $\beta \geq 1$ appear intractable. However, they can still be analysed by assuming a scaling form for the bosonic self-energy,

$$\Pi(\mathrm{i}\Omega_m) - \Pi(0) \sim -c_B |\Omega_m|^{\eta'}, \tag{2.26}$$

where $\eta'$ will be fixed self-consistently at the end of the calculation. At low frequencies, if $\eta < 2$, the bosonic propagator reads

$$D(\mathrm{i}\Omega_m, \boldsymbol{q}) \simeq \frac{1}{\boldsymbol{q}^2 + c_B |\Omega_m|^{\eta'}}. \tag{2.27}$$

Otherwise, the frequency dependence from self-energies is subleading, and

$$D(\mathrm{i}\Omega_m, \boldsymbol{q}) \simeq \frac{1}{\Omega_m^2 + \boldsymbol{q}^2}. \tag{2.28}$$

[1] A non-zero $\beta$ requires $m \geq 2$, but the scaling behaviour obtained below remains valid even for $m = 1$; further details are provided in present in Appendix B.

In either case, the propagator may be written uniformly as

$$D(\mathrm{i}\Omega_m, \boldsymbol{q}) \simeq \frac{1}{\boldsymbol{q}^2 + c_B|\Omega_m|^\eta}, \tag{2.29}$$

with the requirement that $\eta \leq 2$.

Therefore, both fermion and boson self-energies take the form

$$\begin{aligned}\mathcal{I}^d_{\alpha,\beta}(\mathrm{i}x) \equiv & \int_{-\infty}^{\infty} \left( \prod_{i=1}^{\alpha} \frac{d\omega_i}{2\pi} d\xi_{\boldsymbol{k}_i} \frac{1}{\mathrm{isgn}(\omega_i)\Gamma/2 - \xi_{\boldsymbol{k}_i}} \right) \\ & \times \left( \int_{-\infty}^{\infty} \prod_{j=1}^{\beta-1} \frac{d\Omega_j}{2\pi} \int_0^{\infty} \frac{d^d\boldsymbol{q}_j}{(2\pi)^2} \frac{1}{c_B|\Omega_j|^\eta + \boldsymbol{q}_j^2} \right) \int_0^{\infty} \frac{d^d\boldsymbol{q}_\beta}{(2\pi)^2} \frac{1}{c_B|x + \sum_{j=1}^{\beta-1}\Omega_j + \sum_{i=1}^{\alpha}\omega_i|^\eta + \boldsymbol{q}_\beta^2}.\end{aligned} \tag{2.30}$$

Such an integral, in fact, can be evaluated by dimensional counting.

**Yukawa coupling** To begin with, let us consider the simplest case as an example, where $m = n = 1$. For boson self-energy, $\alpha = 2$ and $\beta = 0$, so

$$\Pi_{m=n=1}(\mathrm{i}\Omega) \sim \int_{-\infty}^{\infty} \frac{d\omega}{2\pi} d\xi_{\boldsymbol{k}_1} d\xi_{\boldsymbol{k}_2} \frac{1}{\mathrm{isgn}(\omega)\Gamma/2 - \xi_{\boldsymbol{k}_i}} \frac{1}{\mathrm{isgn}(\omega+\Omega)\Gamma/2 - \xi_{\boldsymbol{k}_2}}. \tag{2.31}$$

Now let us analyse this equation step by step.

1. The function $\mathrm{sgn}(\omega)$ does not contain any explicit frequency scaling dependence. Consequently, the integrals $\int d\xi_{\boldsymbol{k}_1}$ and $\int d\xi_{\boldsymbol{k}_2}$ brings a number whose dimension is $[\text{frequency}]^0$.

2. The frequency integral $\int d\omega$ will yields a final result of dimension $[\text{frequency}]^1$.

3. There will be a constraint from $\mathrm{sgn}(\omega)$ and $\mathrm{sgn}(\Omega+\omega)$, such that $\omega \in [0, |\Omega|]$. So we *suggest* that the final answer of eqn.(2.31) should be

$$\Pi_{m=n=1}(\mathrm{i}\Omega) \equiv c_B|\Omega| \sim |\Omega|. \tag{2.32}$$

This result precisely matches the computation in ref.[8]. Similarly, for fermion self-energy in this case, one obtains

$$\Sigma_{m=n=1}(\mathrm{i}\omega) = \int_{-\infty}^{\infty} \frac{d\omega'}{2\pi} d\xi_{\boldsymbol{k}_i} \frac{1}{\mathrm{isgn}(\omega')\Gamma/2 - \xi_{\boldsymbol{k}}} \int_0^{\infty} \frac{d^d\boldsymbol{q}}{(2\pi)^2} \frac{1}{c_B|\omega+\omega'| + \boldsymbol{q}_\beta^2}. \tag{2.33}$$

The analysis is similar.

1. Again, $\int d\xi_{\boldsymbol{k}}$ will not bring any scaling behaviour.

2. The boson momentum integral $\int d^d\boldsymbol{q}$ results in a term of dimension $[\text{frequency}]^{(d-2)/2}$.

3. With $\int d\omega'$, the final result will be of dimensions $[\text{frequency}]^{1+(d-2)/2} = [\text{frequency}]^{d/2}$.

4. Considering the constraint on integration domain from $\mathrm{sgn}(\omega')$, we conclude

$$\Sigma_{m=n=1}(\mathrm{i}\Omega) \equiv c_F|\Omega|^{d/2} \sim |\Omega|^{d/2}. \tag{2.34}$$

This agrees with the precise computation in refs.[8, 11] as well.

**General coupling** With examples above, we can generalise the analysis to eqn.(2.30).

1. Still, $\int d\xi_{\boldsymbol{k}}$ is irrelevant, so its result is of dimension zero, $[x]^0$.
2. Each $\int d^d\boldsymbol{q}$ brings a term of dimension $[x]^{(d-2)\eta/2}$, and there are $\beta$ integrals over boson momentum. Hence, one obtain a term of dimension $[x]^{(d-2)\eta\beta/2}$.
3. There are $(\alpha+\beta-1)$ integrals over frequencies, which contribute in total a dimension $[x]^{\alpha+\beta-1}$.
4. The final result should be of dimension $[x]^{\alpha+\beta-1+(d-2)\eta\beta/2}$.
5. Due to the constraint on integration domain, we can deduce that eqn.(2.30) takes the form

$$\mathcal{I}^d_{\alpha,\beta}(\mathrm{i}x) \sim x^{\alpha+\beta-1+\frac{(d-2)\eta}{2}\beta}. \tag{2.35}$$

To confirm this dimension analysis above, let us move on to the explicit evaluation on eqn.(2.30).

### 2.2.2 Explicit Evaluation of the Self-Energies

Using Eqs. (A.2) and (A.3), we evaluate the scaling behaviour of the generic self-energy diagram,

$$\begin{aligned}\mathcal{I}^d_{\alpha,\beta}(\mathrm{i}x) \equiv& \int_{-\infty}^{\infty}\left(\prod_{i=1}^{\alpha}\frac{d\omega_i}{2\pi}d\xi_{\boldsymbol{k}_i}\frac{1}{\mathrm{isgn}(\omega_i)\Gamma/2-\xi_{\boldsymbol{k}_i}}\right)\\ &\times\left(\int_{-\infty}^{\infty}\prod_{j=1}^{\beta-1}\frac{d\Omega_j}{2\pi}\int_0^{\infty}\frac{d^d\boldsymbol{q}_j}{(2\pi)^2}\frac{1}{c_B|\Omega_j|^{\eta}+\boldsymbol{q}_j^2}\right)\int_0^{\infty}\frac{d^d\boldsymbol{q}_\beta}{(2\pi)^2}\frac{1}{c_B|x+\sum_{j=1}^{\beta-1}\Omega_j+\sum_{i=1}^{2n}\omega_i|^{\eta}+\boldsymbol{q}_\beta^2}\\ \sim& (-\mathrm{i})^{\alpha}\int_{-\infty}^{\infty}\left(\prod_{j=1}^{\beta-1}d\Omega_j|\Omega_j|^{\frac{\eta(d-2)}{2}}\right)\left|x+\sum_{j=1}^{\beta-1}\Omega_j\right|^{\frac{\eta(d-2)}{2}+\alpha}.\end{aligned} \tag{2.36}$$

We perform the change of variables $\Omega_j \equiv x\cdot u_j$ so that $d\Omega_j = xdu_j$. The integral (2.36) then scales as

$$\mathcal{I}^d_{\alpha,\beta}(\mathrm{i}x) \sim (-\mathrm{i})^{\alpha}x^{\alpha+\beta+\frac{\eta(d-2)}{2}-1+\frac{\eta(d-2)(\beta-1)}{2}}, \tag{2.37}$$

which is precisely the result we have found via dimensional analysis, eqn.(2.35).

For bosonic self-energy, we identify $\alpha = 2n$ and $\beta = m - 1$; for fermionic self-energy, $\alpha = 2n - 1$ and $\beta = m$[2]. This yields

$$\Pi(\mathrm{i}\Omega) - \Pi(0) \sim -c_B g^2 \Omega^{2n+m-2+\frac{\eta(d-2)(m-1)}{2}}, \tag{2.38}$$

$$\Sigma(\mathrm{i}\omega) \sim -\mathrm{i}c_F g^2 \omega^{2n+m-2+\frac{\eta(d-2)m}{2}}, \tag{2.39}$$

where $c_B$ and $c_F$ constants not relevant for scaling analysis.

Now let us determine $\eta$ by imposing self-consistency on the assumed scaling, $\Pi(\mathrm{i}\Omega_m) - \Pi(0) \sim -c_B|\Omega_m|^{\eta'}$.

- **case i:** If $\eta' < 2$, then $\eta = \eta'$, and $\eta$ satisfies

$$2n + m - 2 + \frac{\eta(d-2)}{2} + \frac{\eta(d-2)(m-2)}{2} = \eta. \tag{2.40}$$

  Solving for $\eta$, one finds

$$\eta = -\frac{2(m+2n-2)}{dm - d - 2m}. \tag{2.41}$$

  Substituting this back into the self-energies (2.38) and (2.39), we have

$$\Pi(\mathrm{i}\Omega) - \Pi(0) \sim -c_B g^2 \Omega^{-\frac{2(m+2n-2)}{d(m-1)-2m}}, \tag{2.42}$$

$$\Sigma(\mathrm{i}\omega) \sim -\mathrm{i}c_F g^2 \omega^{-\frac{d(m+2n-2)}{d(m-1)-2m}}. \tag{2.43}$$

  For this solution to be consistent, the exponent must satisfy

$$-\frac{2(m+2n-2)}{d(m-1)-2m} < 2. \tag{2.44}$$

- **case ii:** If $\eta' \geq 2$, then $\eta = 2$, yielding

$$\Pi(\mathrm{i}\Omega) - \Pi(0) \sim -c_B g^2 \Omega^{2n+m-2+(d-2)(m-1)}, \tag{2.45}$$

$$\Sigma(\mathrm{i}\omega) \sim -\mathrm{i}c_F g^2 \omega^{2n+m-2+(d-2)m}, \tag{2.46}$$

  with the consistency condition

$$2n + m - 2 + (d-2)(m-1) \geq 2. \tag{2.47}$$

## 3 Conductivity

### 3.1 The unique approach to linearity

Having obtained the propagators and self-energies, we now estimate the conductivity using the *Kubo formula*,

$$\sigma^{\mu\nu}(\mathrm{i}\Omega_m) = -\frac{1}{\Omega_m}\left[\tilde{\Pi}^{\mu\nu}(\Omega)\right]_{\Omega=0}^{\Omega=\mathrm{i}\Omega_m} \tag{3.1}$$

[2]Our result also captures the feature of models with $m = 1$, and the explicit calculation for $m = 1$ is given in App.B

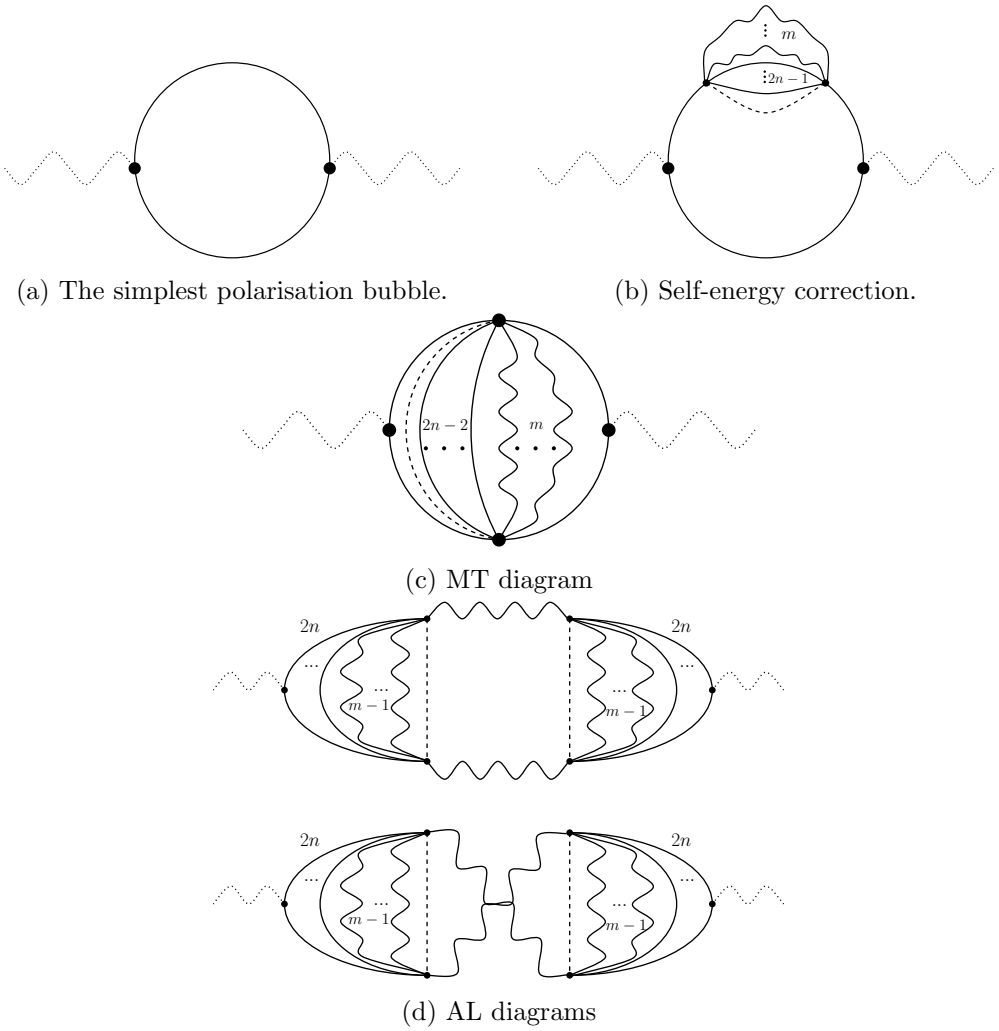


(a) The simplest polarisation bubble.

(b) Self-energy correction.

(c) MT diagram

(d) AL diagrams

**Figure 2**: Polarisation diagrams. The solid line represents the "bare" propagator (2.24).

where $\tilde{\Pi}^{\mu\nu}$ denotes the current-current correlator, or equivalently, the polarisation bubble for the external electromagnetic field. Since we consider only electric fields in this work, $\tilde{\Pi}^{\mu\nu}$ is diagonal.

The polarisation bubble receives contributions from the simplest one-loop diagram, as well as from self-energy insertions and vertex corrections, as illustrated in Fig. 2. To leading order, the polarisation is illustrated in Fig. 2a, and is given by [21]

$$\begin{aligned}
&\tilde{\Pi}_0^{\mu\nu}(\mathrm{i}\Omega_m) \\
&= -\frac{2}{m^2} T \sum_n \int \frac{d^d \boldsymbol{k}}{(2\pi)^2} k^\mu k^\nu \frac{1}{\mathrm{i}\omega_n - \frac{\boldsymbol{k}^2}{2m} + \mu + \mathrm{i}\Gamma \mathrm{sgn}(\omega_n)/2} \frac{1}{\mathrm{i}(\omega_n + \Omega_m) - \frac{\boldsymbol{k}^2}{2m} + \mu + \mathrm{i}\Gamma \mathrm{sgn}(\omega_n + \Omega_m)/2} \\
&\simeq -v_F^2 \mathcal{N} \delta^{\mu\nu} \frac{\Omega_m}{\Omega_m + \mathrm{sgn}(\Omega_m)\Gamma},
\end{aligned} \tag{3.2}$$

which leads to a finite constant residual resistivity. Here we have assumed that the domi-

nant contributions come from fermions near the Fermi surface [21].

At the next order, the polarisation receives corrections from the fermionic self-energy, shown in Fig. 2b. For convenience, we write the self-energy in the form

$$\Sigma(\mathrm{i}\omega) \equiv -\mathrm{i}c_F g^2 \omega^{\varsigma}. \tag{3.3}$$

The corresponding correction to the polarisation tensor is

$$\begin{aligned}\tilde{\Pi}_g^{\mu\nu}(\mathrm{i}\Omega) \sim & -\frac{2k_F^2\mathcal{N}}{m^2}\delta^{\mu\nu}\int \frac{d\omega_n}{2\pi}d\xi_{\boldsymbol{k}}\frac{1}{\mathrm{i}\omega_n - \xi_{\boldsymbol{k}} + \mathrm{i}\Gamma\mathrm{sgn}(\omega)/2}\frac{1}{\mathrm{i}\omega_n - \xi_{\boldsymbol{k}} + \mathrm{i}\Gamma\mathrm{sgn}(\omega)/2} \\ & \times\frac{1}{\mathrm{i}(\omega+\Omega) - \xi_{\boldsymbol{k}} + \mathrm{i}\Gamma\mathrm{sgn}(\omega+\Omega)/2}\left(-\mathrm{i}c_F g^2\omega^{\varsigma}\right) \\ \sim & \; g^2\delta^{\mu\nu}\Omega^{\varsigma+1}\end{aligned} \tag{3.4}$$

at low frequencies.

The vertex corrections—specifically, the Maki-Thompson (MT) diagram (Fig.2c) and the Aslamazov-Larkin (AL) diagrams (Fig.2d), vanish in our model. This cancellation arises because the disorder average enforces spatial locality, effectively decoupling all momenta in the internal propagators via a delta function in position space [8]. Take the MT diagram as an example: after disorder averaging, it yields

$$\tilde{\Pi}_{\mathrm{MT}}(\mathrm{i}\Omega) \sim \int d^2\boldsymbol{k}d^2\boldsymbol{k}'\boldsymbol{k}\boldsymbol{k}'G(\boldsymbol{k},\mathrm{i}\omega)G(\boldsymbol{k},\mathrm{i}(\omega+\Omega))G(\boldsymbol{k}',\mathrm{i}\omega')G(\boldsymbol{k}',\mathrm{i}(\omega'+\Omega))..., \tag{3.5}$$

where the integrand is odd under both $\boldsymbol{k}\to-\boldsymbol{k}$ and $\boldsymbol{k}'\to-\boldsymbol{k}'$, and thus integrates to zero. The same argument applies to the AL diagrams. As a result, all vertex corrections vanish in these SYK-rised models.

Having computed all relevant polarisation tensors, we now apply the Kubo formula to extract the resistivity. Denoting the self-energy correction to the polarisation as $\tilde{\Pi}_g \equiv -c_g g^2\Omega^{1+\varsigma}$, where $c_g$ is a constant, the total polarisation tensor to order $\mathcal{O}(g^2)$ reads

$$\tilde{\Pi}^{\mu\nu} \simeq \tilde{\Pi}_0^{\mu\nu} + \tilde{\Pi}_g^{\mu\nu}. \tag{3.6}$$

Substituting into the Kubo formula (3.1) and analytically continuing ($\mathrm{i}\Omega\to\Omega$), we obtain the conductivity

$$\sigma^{\mu\nu}(\Omega) = v_F^2\mathcal{N}\delta^{\mu\nu}\frac{1}{\Gamma - \mathrm{i}\Omega} - c_g g^2\delta^{\mu\nu}(-\mathrm{i}\Omega)^{\varsigma}. \tag{3.7}$$

In the absence of a magnetic field, the tensor structure is trivial and $\tilde{\Pi}$ is diagonal, so we drop the indices and write the scalar conductivity. Taking the inverse and extracting the real part, the resistivity is

$$\mathrm{Re}\,\rho = \mathrm{Re}\,\frac{1}{\sigma} \sim \frac{2\Gamma}{\mathcal{N}v_F^2} + g^2 c_g'\Omega^{\varsigma}, \tag{3.8}$$

where $c_g'$ absorbs numerical prefactors independent of $g^2$.

The frequency dependence at zero temperature translates to $T$-dependence at finite temperature. Our goal is to identify all combinations of $d, m, n$ that yield a linear resistivity. For $\eta < 2$, it corresponds to solving the equation

$$\varsigma = -\frac{d(m+2n-2)}{d(m-1)-2m} = 1, \tag{3.9}$$

or

$$d(m+2n-2) = 2m - d(m-1), \tag{3.10}$$

which can be rearranged as

$$n = \left(\frac{1}{d} - 1\right) m + \frac{3}{2} \in \mathbb{Z}^+. \tag{3.11}$$

There is no solution for $d = 1$, and we focus on $d \geq 2$. As $n, m \in \mathbb{Z}^+$, we also impose

$$0 < m \leq \frac{1}{2}\frac{d}{d-1}. \tag{3.12}$$

The only integer $m$ satisfying this is $m = 1$ when $d = 2$. Substituting $d = 2$ and $m = 1$ into eqn.(3.11) gives $n = 1$. One can further verify that when $n = m = 1$ and $d = 2$, $\Pi \sim \Omega$, consistent with the assumption.

For $\eta = 2$ (or $\eta' \geq 2$), we need to solve

$$\varsigma = 2n + m - 2 + (d-2)m = 1. \tag{3.13}$$

When $d = 2$, the only solution is $n = m = 1$, but this leads to $\Pi \sim \Omega$, implying $\eta' = 1$, which contradicts the assumption $\eta' \geq 2$. Thus, it cannot be a valid solution for $\eta = 2$. For higher dimensions, since $2n - 2 \geq 0$ and $m + (d-2)m \geq 2m \geq 2$, the left-hand side of eqn.(3.13) is always greater than or equal to 2. Consequently, there are no consistent integer solutions yielding linear resistivity for $\eta = 2$.

Readers may notice that eqns.(3.7) and (3.8) differ from the results in ref.[8], where a logarithmic term $\ln(\Omega)$ appears but is absent here. This apparent discrepancy originates from the scaling approximation used in integral (A.2), which cannot capture logarithmic corrections. Instead, it yields a constant term when $d = 2$. A direct, detailed calculation, rather than a general scaling analysis, naturally recovers the $\ln(\Omega)$ behaviour. Such a calculation for the case $d = 2$ is presented in Appendix C.

In summary, *the only consistent choice yielding linear resistivity is* $d = 2$ *with* $n = m = 1$, precisely corresponding to the Yukawa-type coupling studied in ref. [8].

## 4 Spatially Uniform Model

This section will illustrate that sptatially uniform coupling between FS and critical bosons can never yield linear resistivity. To be precise, we consider the same model, while the coupling parameter has no spatial dependence. That is,

$$S_g = \frac{g_{\{i\}\{j\}\{l\}}}{N^{(2n+m-1)/2}} \int d\tau d^d r \sum_{\{i\},\{j\},\{l\}} \psi^\dagger_{i_1,\boldsymbol{k}}(\boldsymbol{r},\tau)...\psi^\dagger_{i_n,\boldsymbol{k}}(\boldsymbol{r},\tau) \times \psi_{j_1,\boldsymbol{k}+\boldsymbol{q}}(\boldsymbol{r},\tau)...\psi_{j_n,\boldsymbol{k}+\boldsymbol{q}}(\boldsymbol{r},\tau)\phi_{l_1,\boldsymbol{q}}(\boldsymbol{r},\tau)...\phi_{l_m,\boldsymbol{q}}(\boldsymbol{r},\tau), \tag{4.1}$$

with

$$\langle g_{\{i\}\{j\}\{l\}} \rangle = 0, \tag{4.2}$$

$$\langle g_{\{i\}\{j\}\{l\}} g^*_{\{i'\}\{j'\}\{l'\}} \rangle = g^2 \delta_{\{i\}\{i'\},\{j\}\{j'\},\{l\}\{l'\}}. \tag{4.3}$$

Firstly, without potential disorder, the system shows a vanishing resistivity due to the 'boson drag' [20], so random couplings (4.1) without potential disorderr have been ruled out at the beginning.

Due to momentum conservation, the integral (2.36) becomes

$$\mathfrak{I}^d_{\alpha,\beta}(\mathrm{i}x,\boldsymbol{y}) \equiv \int_{-\infty}^{\infty} \left( \prod_{i=1}^{\alpha-1} \frac{d\omega_i}{2\pi} \frac{d^d\boldsymbol{k}_i}{(2\pi)^d} \frac{1}{\mathrm{isgn}(\omega_i)\Gamma/2 - \xi_{\boldsymbol{k}_i}} \right) \left( \int_{-\infty}^{\infty} \prod_{j=1}^{\beta} \frac{d\Omega_j}{2\pi} \int_0^{\infty} \frac{d^d\boldsymbol{q}_j}{(2\pi)^2} \frac{1}{c_B|\Omega_j|^\eta + \boldsymbol{q}_j^2} \right) \times \frac{1}{\mathrm{isgn}(x + \sum_{j=1}^{\beta}\Omega_j + \sum_{i=1}^{\alpha-1}\omega_i)\Gamma/2 - \xi_{\sum_{i=1}^{\alpha-1}\boldsymbol{k}_i + \sum_{i=1}^{\beta}\boldsymbol{q}_i + \boldsymbol{y}}}. \tag{4.4}$$

The integral $\int d^d\boldsymbol{q}$ should be decomposed into $\int d\theta$ and $\int qdq$, and the scattering angles $\theta_i$ will appear in $\xi_{\sum_{i=1}^{\alpha-1}\boldsymbol{k}_i + \sum_{i=1}^{\beta}\boldsymbol{q}_i + \boldsymbol{y}}$ after expansion. The total integral is difficult to be computed analytically, so we apply the same dimensional analysis above.

1. The disorder scattering rate $\Gamma$ is the largest scale in our system, so the angular integral can be neglected, together with the $q$-dependence in these terms. Consequently, $\int d\theta$ brings a term of $[x]^0[q]^0$.

2. The integrals $\int d\xi_{\boldsymbol{k}}$ are again irrelevant in bringing any scaling behaviour, whereas the integrals $\int d^d\boldsymbol{q}$ will result in a term with dimension $[x]^{\eta(d-2)/2}$.

3. The frequency integrals, $\int d\omega_i$ and $\int d\Omega_j$ together yield a dimension of $[\text{frequency}]^{\alpha+\beta-1}$.

4. Finally, the domain of $\omega_i$ and $\Omega_j$ will be limited within $[0, |x|]$. One finds

$$\mathfrak{I}^d_{\alpha,\beta}(\mathrm{i}x,\boldsymbol{y}) \sim x^{\alpha+\beta+\frac{\beta\eta(d-2)}{2}-1}, \tag{4.5}$$

This is precisely the same scaling behaviour with $\mathcal{I}^d_{\alpha,\beta}(\mathrm{i}x,\boldsymbol{y})$, given by eqn.(2.37).

So at the level of self-energies, the spatial independent model (4.4) has the same scaling behaviour with spatially random model (2.5). According to eqn.(3.7), the leading-order conductivity from $\tilde{\Pi}_g^{\mu\nu}$ will inherit the freqency-dependence from electron self-energy, so a self-energy that satisfies $\Sigma \sim \omega$ will yield a linear conductivity. However, a spatially uniform system admits vertex corrections, MT diagram and AL diagrams. Therefore, the self-energy alone is not enough the capture the correct transport properties. Meanwhile, vertex corrections will only bring terms, whose order is no lower than the electron self-energy, so the minimum condition of model (4.4) to reproduce a linear resistivity is that $\Sigma \sim \omega^{\square}$ with $\square \leq 1$.

Applying the same analysis in sec.3, we conclude that only $d = 2$ and $m = n = 1$ can give us electron self-energy linear in frequency, and increasing dimensions or number of the fields will increase the value of $\square$ as well. Therefore, $\Sigma \sim \omega$ is the lowest order one can obtain from the interaction (4.1) in $d \geq 2$, and the spatially uniform model with $m = n = 1$ in 2D is the only candidate of strange metals in this family.

However, the linear contribution from electron self-energy will be canceled by MT diagrams [8, 20], whereas the AL will bring higher order terms. The only candidate is also ruled out, so the interaction (4.1) can never give rise to a linear resistivity.

Combining what we have found in sec.3, one reaches the conclusion that only 2D spatially random Yukawa coupling (1.1) is able to reproduce strange-metal transport.

## 5 Conclusion

In this work, we have systematically explored the full class of SYK-rised interactions of the form $(\psi^\dagger\psi)^n\phi^m$, involving multiple fermions and scalar bosons, as potential candidate theories for strange metals, across arbitrary dimensions $d \geq 2$. It turns out that only spatially random Yukawa-type interactions ($n = m = 1$) in two dimensions lead to linear-$T$ resistivity. There is no other candidate of strange metals within this SYK-rised class. Our analysis reveals that only the Yukawa-type coupling with $n = m = 1$ in two spatial dimensions yields a linear-in-temperature resistivity. No other combination within this interaction class leads to such scaling, making the 2D Yukawa model the unique candidate among scalar-coupled SYK-rised theories.

In earlier work [11], we also demonstrated that a spatially random QED-like vector coupling, $\psi^\dagger\nabla^\mu\psi\boldsymbol{a}_\mu$, yields linear resistivity. Here $\boldsymbol{a}$ is a bosonic vector field, not necessarily a gauge field. Taken together, these results suggest that in realistic two-dimensional systems, the random Yukawa and vector couplings serve as minimal building blocks for capturing linear-$T$ resistivity. For any interaction of the form (2.5), the low-temperature resistivity scales as $\rho \sim T^{m+2n-2}$; thus, the linear case arises only when $n = m = 1$, or equivalently from the vector coupling scenario. All higher order terms do not contribute to the linear resistivity. Therefore, there are essentially one class in each category: unique

scalar class and unique vector class.

This paper has focused exclusively on low-temperature linear resistivity in SYK-rised models. While the Yukawa coupling emerges as a viable theory of strange metals within this regime, a more complete understanding requires going beyond the infrared limit. It remains an open question whether SYK-rised models can also account for $H$-linear resistivity and magnetoresistance obeying $H/T$ scaling [22]. These directions will be crucial for determining whether SYK-rised interactions offer a unified framework for understanding the strange metal phase.


## Acknowledgments

The authors would like to thank Ki-Seok Kim, Kyoung-Min Kim, Chao-Jung Lee, Sung-Sik Lee, Yi Zhang for the inspiring discussion. This work is supported by the National Research Foundation of Korea (NRF) grant funded by the Korean government (MSIT) No.NRF-2021R1A2B5B02002603, and No.RS-2023-00218998.


## A Useful Integrals

The following integrals are useful in evaluating self-energies in this article.

- $$\int \frac{x^{d-1}}{A+x^2}dx = \frac{x^d\,{}_2F_1\left(1,\frac{d}{2};\frac{d}{2}+1;-\frac{x^2}{A}\right)}{Ad}, \tag{A.1}$$

  where ${}_2F_1(a,b;c;d)$ is the hypergeometric function.

- $$\int_0^\infty \frac{x^{d-1}}{A+x^2}dx \sim A^{\frac{d-2}{2}}, \tag{A.2}$$

- $$\begin{aligned}
&\int \left(\prod_{i=1}^n dx_i \mathrm{sgn}(x_i)\right)\left|B-\sum_i^n x_i\right|^\lambda \\
&\sim \int_{|\sum_i^n x_i|\le|B|}^\infty \prod_{i=1}^n dx_i \left|B-\sum_i^n x_i\right|^\lambda = \int_{|\sum_i^n x_i|\le|B|}^\infty \prod_{i=1}^n dx_i \left|B-\sum_i^n x_i\right|^\lambda \int dX\delta(X-\sum_i^n x_i) \\
&\sim \int_0^{|B|} d|X| \prod_{i=1}^{n-1}\int_0^{|X|} dx_i \left|B-X\right|^\lambda = \int_0^B dX|X|^{n-1}\left|B-X\right|^\lambda \\
&\sim |B|^{n+\lambda},
\end{aligned} \tag{A.3}$$

## B Self-energies for $m = 1$

As noted in the main text, the integral expression in eqn.(2.36), and hence the resulting self-energies in eqns.(2.38) and (2.39), are formally derived under the assumption $m \geq 2$. In this appendix, we explicitly compute the case $m = 1$ to verify that these expressions remain valid even for $m = 1$.

The bosonic self-energy in $(d+1)$ dimensions takes the form

$$\begin{aligned}
&\Pi(\mathrm{i}\Omega) - \Pi(0) \\
&\simeq -g^2 m \mathcal{N}^{2n} \int \prod_{i=1}^{2n-1} \frac{d\omega_i}{2\pi} d\xi_{\boldsymbol{k}_i} d\xi_{\boldsymbol{k}_{2n}} \frac{1}{\mathrm{isgn}(\omega_i)\Gamma/2 - \xi_{\boldsymbol{k}_i}} \\
&\quad \times \left[ \frac{1}{\mathrm{isgn}(\Omega + \sum_{i=1}^{2n-1} \omega_i)\Gamma/2 - \xi_{\boldsymbol{k}_{2n}}} - \frac{1}{\mathrm{isgn}(\sum_{i=1}^{2n-1} \omega_i)\Gamma/2 - \xi_{\boldsymbol{k}_{2n}}} \right] \\
&\sim -\frac{g^2 m \mathcal{N}^{2n}}{2^{2n}} 2\pi \int \prod_{i=1}^{2n-1} d\omega_i \mathrm{sgn}(\omega_i) \left( \mathrm{sgn}\left( \Omega + \sum_{i=1}^{2n-1} \omega_i \right) - \mathrm{sgn}\left( \sum_{i=1}^{2n-1} \omega_i \right) \right) \\
&\sim |\Omega|^{2n-1},
\end{aligned} \tag{B.1}$$

which agrees with the scaling form of eqn. (2.38) when $m = 1$.

The fermionic self-energy from $g$-coupling is given by

$$\begin{aligned}
\Sigma_g(\mathrm{i}\omega) &= g^2 n \mathcal{N}^{2n-1} \int \left( \prod_{i=1}^{2n-1} \frac{d\omega_i}{2\pi} d\xi_{\boldsymbol{k}_i} \frac{1}{\mathrm{isgn}(\omega_i)\Gamma/2 - \xi_{\boldsymbol{k}_i}} \right) \int_0^\infty \frac{d^d \boldsymbol{q}}{(2\pi)^2} \frac{1}{\boldsymbol{q}^2 + c_B(\omega - \sum_i^{2n-1} \omega_i)^\eta} \\
&\sim g^2 \int \left( \prod_{i=1}^{2n-1} d\omega_i \mathrm{sgn}(\omega_i) \right) \left( \omega - \sum_i^{2n-1} \omega_i \right)^{\frac{\eta(d-2)}{2}} \\
&\sim g^2 \omega^{2n-1+\frac{\eta(d-2)}{d}},
\end{aligned} \tag{B.2}$$

which reproduces the scaling behaviour in eqn. (2.39).

We therefore conclude that eqns. (2.38) and (2.39) correctly capture the scaling behaviour of the self-energies even in the case $m = 1$.

## C Self-energies in Two Dimensions

This section reproduces the logarithmic scaling for $d = 2$ via explicit calculation. This behaviour is not captured by the general result (A.2) used in the main text.

We begin by evaluating the integral

$$J_n(\omega) \equiv \int\limits_{\sum_i^n x_i \le \omega} \left(\prod_{i=1}^n dx_i \mathrm{sgn}(x_i)\right) \ln\left(\left|\omega - \sum_i^n x_i\right|\right)$$
$$\sim \int\limits_{\substack{0 \\ \sum_i^n x_i \le \omega}}^{\infty} \prod_{i=1}^n dx_i \ln\left(\left|\omega - \sum_i^n x_i\right|\right). \tag{C.1}$$

Define $X \equiv \sum_i^n x_i$, and insert it with a delta function,

$$J_n(\omega) \sim \int\limits_{\substack{0 \\ \sum_i^n x_i \le \omega}}^{\infty} \prod_{i=1}^n dx_i \ln\left(\left|\omega - \sum_i^n x_i\right|\right) \int dX \delta(X - \sum_{i=1}^n x_i)$$
$$= \int\limits_{0 \le X \le \omega} dX \int\limits_{\sum_{i=1}^{n-1} x_i \le X} \prod_{i=1}^{n-1} dx_i \ln\Big(\Big|\omega - X\Big|\Big)$$
$$\sim \int_0^\omega dX X^{n-1} \ln(\omega - X). \tag{C.2}$$

The dominant contribution comes from the region near $\omega$, where $\omega \ll 1$, so we expand the integrand as

$$\ln(\omega - X) = \ln(\omega) + \ln\left(1 - \frac{X}{\omega}\right) \simeq \ln(\omega) - \frac{X}{\omega} + \mathcal{O}\left(\frac{X^2}{\omega^2}\right). \tag{C.3}$$

Thus, we find the leading scaling behaviour

$$J_n(\omega) \sim C_1 \omega^n \ln(\omega) + C_2 \omega^n, \tag{C.4}$$

where $C_1$ and $C_2$ are constants.

Now consider the full integral (2.36) in two dimensions:

$$\mathcal{I}^{d=2}_{\alpha,\beta}(\mathrm{i}x) \equiv \int_{-\infty}^{\infty} \left(\prod_{i=1}^{\alpha} \frac{d\omega_i}{2\pi} d\xi_{\boldsymbol{k}_i} \frac{1}{\mathrm{isgn}(\omega_i)\Gamma/2 - \xi_{\boldsymbol{k}_i}}\right)$$
$$\times \left(\prod_{j=1}^{\beta-1} \int_{-\infty}^{\infty} \frac{d\Omega_j}{2\pi} \int_0^\infty \frac{d^2\boldsymbol{q}_j}{(2\pi)^2} \frac{1}{|\Omega_j|^\eta + \boldsymbol{q}_j^2}\right) \int_0^\infty \frac{d^2\boldsymbol{q}_\beta}{(2\pi)^2} \frac{1}{|x + \sum_{j=1}^{\beta-1}\Omega_j + \sum_{i=1}^{2n}\omega_i|^\eta + \boldsymbol{q}_\beta^2}$$
$$\sim (-\mathrm{i})^\alpha \int_{-\infty}^{\infty} \left(\prod_{i=1}^{\alpha} d\omega_i \mathrm{sgn}(\omega_i)\right) \left(\prod_{j=1}^{\beta-1} \int_{-\infty}^{\infty} d\Omega_j \ln\left(\frac{\Lambda_q^2}{|\Omega_j|^\eta}\right)\right) \ln\left(\frac{\Lambda_q^2}{|x + \sum_{j=1}^{\beta-1}\Omega_j + \sum_{i=1}^{2n}\omega_i|^\eta}\right)$$
$$\sim (-\mathrm{i})^\alpha \left(\prod_{j=1}^{\beta-1} \int_{-\infty}^{\infty} d\Omega_j \ln\left(\frac{\Lambda_q^2}{|\Omega_j|^\eta}\right)\right) \left(\left(x + \sum_{j=1}^{\beta-1}\Omega_j\right)^\alpha \left(C_1 \ln\left|x + \sum_{j=1}^{\beta-1}\Omega_j\right| + C_2\right)\right). \tag{C.5}$$

Changing the variables $\{\Omega_i\}$ into $\{u_i\}$, such that

$$\Omega_j \equiv x \cdot u_j \Leftrightarrow d\Omega_j = x du_j, \tag{C.6}$$

one finds

$$\mathcal{I}^{d=2}_{\alpha,\beta}(\mathrm{i}x) \sim (-\mathrm{i})^{\alpha} x^{\alpha+\beta-1} \int \prod_{j=1}^{\beta-1} du_j \ln(x\cdot u_j) \left(1+\sum_{j=1}^{\beta-1} u_j\right)^{\alpha} \ln\left(x\left(1+\sum_{j=1}^{\beta-1} u_j\right)\right)$$
$$\sim (-\mathrm{i})^{\alpha} x^{\alpha+\beta-1} \sum_{\iota=0}^{\beta} c_\iota (\ln x_i)^{\iota}. \tag{C.7}$$

The coefficient $c_i$ is fixed by explicit computation, but being $x$-independent, can remain unspecified in a qualitative analysis.

In particular, for the bosonic self-energy, $\alpha = 2n$ and $\beta = m-1$, and for electronic self-energy, $\alpha = 2n-1$ and $\beta = m$. We thus arrive at the general expressions in $d = 2$,

$$\Pi(\mathrm{i}\Omega) - \Pi(0) = -g^2 \Omega^{2n+m-2} \sum_{i=0}^{m-1} c_i (\ln(\Omega))^i, \tag{C.8}$$

$$\Sigma(\mathrm{i}\omega) = -\mathrm{i}g^2 \omega^{2n+m-2} \sum_{i=0}^{m} c_i (\ln(\omega))^i. \tag{C.9}$$

These results demonstrate explicitly that the logarithmic scaling, absent in the hypergeometric estimate, is correctly reproduced by direct evaluation in two dimensions. Taking $m = n = 1$, we can recover the results in ref.[8].

## D A detour: the failure of Fermi's golden rule

Beyond resistivity scaling, our study also uncovers the breakdown of Fermi's Golden Rule in disordered models, even in cases where quasiparticles remain well-defined.

Let us detour to the failure of Fermi's golden rule in SYK-rised models. According to the analysis in ref.[11], Fermi's Golden Rule can help to understand the emergence of linearity from the spatial random coupling (1.1), depite the absence of well-defined quasiparticles. In both scalar and vector models, the bosonic self-energy takes the form $\Pi(\Omega) \sim C_b \Omega$, where $C_d$ is a constant, leading to a bosonic dispersion $\Omega \sim \boldsymbol{q}^2$. In $(d+1)$-dimensional systems, Bosonic density of states contributes a $T^{d/2}$-dependence to the resistivity. Meanwhile, the angular correction factor $(1-\cos\theta)$, with $\theta$ the scattering angle, is temperature-independent due to the relaxation of momentum conservation at each interaction vertex. Consequently, at low temperature, both interactions produce linear resistivity, though the linearity arises from different polarisation bubbles in Kubo formula [11].

In our generalised model (2.5), the bosonic dispersion relation takes the form

$$\Omega \sim \boldsymbol{q}^{2/\eta} \equiv \boldsymbol{q}^{\alpha}, \tag{D.1}$$

where

$$\alpha = \begin{cases} -\dfrac{d(m-1)-2m}{m+2n-2}, & \eta' < 2 \\ 1, & \eta' \geq 2 \end{cases} \tag{D.2}$$

as implied by the bosonic dispersion from (2.42).

**Golden Rule estimate** According to Fermi's golden rule, the lifetime of an electron is estimated as

$$\begin{aligned}\frac{1}{\tau} &\sim \int \prod_{i=1}^{2n-1} d^d\boldsymbol{k}_i\, f_{\boldsymbol{k}_i} \prod_{j=1}^{m} d^d\boldsymbol{q}_j\, b_{\boldsymbol{q}_j} (1-\cos\theta)\, \delta\left(\sum_{i=1}^{2n-1}\omega_i + \sum_{j=1}^{m}\Omega_j - \omega_{2n}\right) \\ &\sim \int \prod_{i=1}^{2n-1} d\omega_i \frac{1}{e^{\beta\omega_i}+1} \prod_{j=1}^{m} d\Omega_j \frac{1}{e^{\beta\Omega_j}-1}\Omega_j^{\frac{d}{\alpha}-1}(1-\cos\theta)\, \delta\left(\sum_{i=1}^{2n-1}\omega_i + \sum_{j=1}^{m}\Omega_j - \omega_{2n}\right),\end{aligned} \tag{D.3}$$

where $f_{\boldsymbol{k}}$ and $b_{\boldsymbol{k}}$ are the Fermi-Dirac and Bose-Einstein distribution functions. In second step, we have changed variables from momenta to frequencies using despersion relation (D.1). Rescaling variables as $x_i \equiv \beta\omega_i$, $y_j \equiv \beta\Omega_j$, and $z = \beta\omega_{2n-1}$, we find

$$\frac{1}{\tau}_{\text{GR}} \sim T^{m\frac{d}{\alpha}+2n-2} \int \prod_{i=1}^{2n-2} dx_i \frac{1}{e^{x_i}+1} \prod_{j=1}^{m} dy_j \frac{1}{e^{y_j}-1}\frac{1}{e^{z}+1}(1-\cos\theta). \tag{D.4}$$

**Kubo Formula calculation** Meanwhile, the resistivity (3.8) derived from the Kubo formula scales as

$$\rho_{\text{Kubo}} \sim T^{\varsigma} \tag{D.5}$$

(from eqns. (2.43) and (2.46)), where

$$\varsigma = \begin{cases} -\dfrac{d(m+2n-2)}{d(m-1)-2m} = \dfrac{d}{\alpha}, & \eta' < 2 \\ 2n+m-2+(d-2)m, & \eta' \geq 2 \end{cases}. \tag{D.6}$$

We see that the golden rule fails to reproduce the correct scaling: the result (D.4) does not match the Kubo-derived scaling (D.6), except in the special case $m = n = 1$, where the two estimates coincide [11]. Remarkably, this agreement occurs despite the absence of well-defined quasiparticles in two dimensions.

Admittedly, existence of well-defined quasiparticles, characterised by $\Sigma \sim \omega^{\varsigma}$ with $\varsigma \geq 2$, is a necessary condition for the applicability of the golden rule. In fact, there are no well-defined quasiparticles when $\eta < 2$. To see this, consider the case with $n + m > 2$, and distinguish two regimes within it:

i. If $\eta' = \eta < 0$, then $\varsigma = \eta d/2 < 0 < 2$ (according to eqn. (2.43)). This outlaws the existence of quasiparticles.

ii. For $0 < \eta' = -2(m+2n-2)/[d(m-1)-2m] < 2$, the condition

$$0 < d < \frac{m-2n+2}{m-1} \leq \frac{m}{m-1} \leq 2, \tag{D.7}$$

is required, with $m > 1$. However, since $d \geq 2$, this condition cannot be met.

again ruling out well-defined quasiparticles. Thus, in the regime $\eta < 2$, the absence of quasiparticles can naturally explains why the golden rule fails.

However, the golden rule fails in SYK-rised models even when quasiparticles are present. When $\eta' > 2$, quasiparticles may exist. In this case, the fermionic exponent is $\varsigma = \eta' + d - 2$, since $\eta' = 2n + m - 2 + (d-2)(m-1)$ according to (2.45). If $\varsigma \geq 2$ (e.g.$m = n = 2$and $d = 3$), the quasiparticles are well-defined. However, even in this regime, the golden rule does not yield the correct scaling of resistivity.

As discussed in the previous section, momentum conservation is relaxed at each interaction vertex due to disorder averaging. This decouples spatial momentum across different interaction lines. It is therefore highly likely that the golden rule, which relies on well-defined scattering kinematics, fails to correctly estimate the resistivity in SYK-rised models, even in the presence of quasiparticles. The mechanisms governing when the golden rule applies or fails in SYK-rised models remain unknown and deserve further investigation.

## References


[1] P.A. Lee, N. Nagaosa and X.-G. Wen, *Doping a mott insulator: Physics of high-temperature superconductivity*, *Rev. Mod. Phys.* **78** (2006) 17.

[2] P.W. Anderson, *The theory of superconductivity in the high-$T_c$ cuprates*, Princeton University Press (2017).

[3] S.-S. Lee, *Recent Developments in Non-Fermi Liquid Theory*, *Ann. Rev. Condensed Matter Phys.* **9** (2018) 227 [1703.08172].

[4] R.L. Greene, P.R. Mandal, N.R. Poniatowski and T. Sarkar, *The strange metal state of the electron-doped cuprates*, *Annual Review of Condensed Matter Physics* **11** (2020) 213 [https://doi.org/10.1146/annurev-conmatphys-031119-050558].

[5] C.M. Varma, *Colloquium: Linear in temperature resistivity and associated mysteries including high temperature superconductivity*, *Rev. Mod. Phys.* **92** (2020) 031001.

[6] S.A. Hartnoll and A.P. Mackenzie, *Colloquium: Planckian dissipation in metals*, *Rev. Mod. Phys.* **94** (2022) 041002 [2107.07802].

[7] P.W. Phillips, N.E. Hussey and P. Abbamonte, *Stranger than metals*, *Science* **377** (2022) abh4273 [2205.12979].

[8] A.A. Patel, H. Guo, I. Esterlis and S. Sachdev, *Universal theory of strange metals from spatially random interactions*, *Science* **381** (2023) abq6011 [2203.04990].

[9] S.-J. Sin and Y.-L. Wang, *ER=EPR and Strange Metals from Quantum Entanglement*, 2503.19431.

[10] J. Maldacena and L. Susskind, *Cool horizons for entangled black holes*, *Fortsch. Phys.* **61** (2013) 781 [1306.0533].

[11] Y.-L. Wang, X.-H. Ge and S.-J. Sin, *Linear-T resistivity from spatially random vector coupling*, *Phys. Rev. B* **111** (2025) 115135 [2406.11170].

[12] Y.-L. Wang, Y.-K. Han, X.-H. Ge and S.-J. Sin, *Hall Angle of a Spatially Random Vector Model*, 2501.07792.

[13] S. Sachdev and J. Ye, *Gapless spin-fluid ground state in a random quantum heisenberg magnet*, *Phys. Rev. Lett.* **70** (1993) 3339.

[14] A. Kitaev, *A simple model of quantum holography*, *Talk at KITP Program: Entanglement in Strongly-Correlated Quantum Matter* (2015) .

[15] D. Chowdhury, A. Georges, O. Parcollet and S. Sachdev, *Sachdev-Ye-Kitaev models and beyond: Window into non-Fermi liquids*, *Rev. Mod. Phys.* **94** (2022) 035004 [2109.05037].

[16] I. Esterlis, H. Guo, A.A. Patel and S. Sachdev, *Large N theory of critical Fermi surfaces*, *Phys. Rev. B* **103** (2021) 235129 [2103.08615].

[17] S.-S. Lee, *Low energy effective theory of Fermi surface coupled with U(1) gauge field in 2+1 dimensions*, *Phys. Rev. B* **80** (2009) 165102 [0905.4532].

[18] J. Cardy, *Scaling and Renormalizationin Statistical Physics*, Cambridge University Press (1996).

[19] Y. Gu, A. Kitaev, S. Sachdev and G. Tarnopolsky, *Notes on the complex Sachdev-Ye-Kitaev model*, *JHEP* **02** (2020) 157 [1910.14099].

[20] H. Guo, A.A. Patel, I. Esterlis and S. Sachdev, *Large-N theory of critical Fermi surfaces. II. Conductivity*, *Phys. Rev. B* **106** (2022) 115151 [2207.08841].

[21] P. Coleman, *Introduction to many-body physics*, Cambridge University Press (2019).

[22] X. Jiang, M. Qin, X. Wei, L. Xu, J. Ke, H. Zhu et al., *Interplay between superconductivity and the strange-metal state in fese*, *Nature Physics* **19** (2023) 365.